Full-Duplex Media-Based Modulation

Yalagala Naresh and A. Chockalingam
Department of ECE, Indian Institute of Science, Bangalore 560012

***Abstract*—Media-based modulation (MBM) is an attractive modulation scheme that offers MIMO benefits by placing digitally controlled parasitic elements as radio frequency (RF) mirrors near the transmit antenna. Different realizations of the ON/OFF status of these mirrors result in different channel fades which constitute the channel modulation alphabet. In this paper, we investigate full-duplex (FD) communication using MBM. First, we study full-duplex MBM (FD-MBM) scheme with full channel state information (CSI). Our numerical results show that, for the same spectral efficiency, FD-MBM outperforms FD with conventional modulation (FD-CM). Next, in order to relax the full CSI assumption, we investigate FD with differential MBM (FD-DMBM) with no CSI/partial CSI, where partial CSI refers to the availability of either self-interference CSI or desired-signal CSI. We propose detectors for the FD-DMBM with no CSI/partial CSI and illustrate their bit error performance.**

Keywords *– Media-based modulation, full-duplex communication, FD-MBM, full/partial CSI, differential MBM, FD-DMBM.*

I. Introduction

Full-duplex (FD) operation is an attractive technique that achieves higher spectral efficiency compared to half-duplex (HD) operation in wireless communications [1]-[5]. In FD systems, a communication node is allowed to transmit and receive simultaneously over the same frequency band, whereas a HD node transmits and receives either in different time slots over the same frequency band or in the same time slot over different frequency bands. FD systems suffer from the high self-interference (SI) due to signal leakage from its own transmitter to the receiver. Several cancellation techniques have been proposed to suppress the SI, which are mainly classified into passive, active analog, and active digital cancellation techniques [6]. Investigations on MIMO FD systems that use multiple transmit and receive antennas in communication nodes have been reported in the literature [7]. Cooperative relay systems with nodes operating in FD mode have also been widely studied [8]-[12].

Most studies on FD systems reported in the literature employ conventional modulation schemes such as QAM/PSK. Some studies have also considered the use of spatial modulation in FD systems [13]-[15]. Recently, a new modulation scheme, termed *media-based modulation (MBM)*, is attracting research attention for wireless communications in rich scattering environments [16]-[19]. A key advantage in MBM over conventional modulation schemes arises from the use of digitally controlled parasitic elements (e.g., varactors, switched capacitors) placed near the transmit antenna as radio frequency (RF) mirrors to achieve high spectral efficiencies. The concept of MBM can be briefly explained as follows.

This work was supported in part by the J. C. Bose National Fellowship, Department of Science and Technology, Government of India.

The RF mirrors placed near the transmit antenna act as RF signal scatterers. Each RF mirror can be digitally switched ON or OFF. A mirror in ON status allows the incident RF signal to pass through transparently, whereas a mirror in OFF status reflects back the incident RF signal. Therefore, the RF mirrors act as controlled scatterers in the propagation environment close to the transmit antenna. The ON/OFF status of the mirrors is called the 'mirror activation pattern' (MAP). If there are m_{rf} mirrors near the transmit antenna, then $2^{m_{rf}}$ MAPs are possible. Because of the ON/OFF control of the mirrors, the propagation environment near the transmit antenna becomes different for different MAPs. This results in different fade realizations for different MAPs. The collection of $2^{m_{rf}}$ such fades corresponding to different MAPs form the MBM channel alphabet. In a given channel use, the transmitter selects one of the $2^{m_{rf}}$ MAPs using m_{rf} input information bits. The transmit antenna transmits a symbol from a conventional modulation alphabet (e.g., QAM) denoted by $\mathbb{A}$. The spectral efficiency of MBM, therefore, is $\eta_{\text{mbm}} = m_{rf} + \log_2 |\mathbb{A}|$ bits per channel use (bpcu). The spectral efficiency increases by 1 bit with the addition of every single RF mirror. This linear increase in spectral efficiency with the number of RF mirrors is an attractive feature in MBM. In addition, it has been also shown that MBM achieves significantly better performance compared to conventional modulation schemes [16]-[21].

In this paper, we investigate full-duplex communication using media-based modulation in a point-to-point setting. We refer to this scheme as FD-MBM scheme. We refer the FD scheme with conventional modulation as FD-CM scheme. Our new contributions can be summarized as follows.

- First, we investigate FD-MBM with full channel state information (CSI) and maximum likelihood detection. Our numerical results show that, for the same spectral efficiency, FD-MBM scheme outperforms FD-CM scheme.
- Next, we relax the full CSI assumption and investigate FD with differential MBM (FD-DMBM) with no CSI/partial CSI, where partial CSI refers to the availability of either self-interference CSI or desired-signal CSI. We propose detectors for the FD-DMBM scheme with no CSI/partial CSI. More specifically, we propose FD-DMBM detectors, namely, (i) desired-signal channel-aware detector that requires only the desired-signal CSI between the two nodes at the receiver, (ii) self-interference channel-aware detector that requires only the self-interference CSI at the receiver, and (iii) channel-unaware detector that does not need any CSI at the receiver for detection. We illustrate the bit error performance of these detectors.

The rest of this paper is organized as follows. The FD-MBM

system is presented in Section II. Section III presents the FD-DMBM system and the proposed three detectors. Section IV presents the results and discussions. Conclusions and potential for future work are presented in Section V.

II. FD-MBM System

In this section, we present the FD-MBM system model. Consider FD communication between two nodes (node 1 and node 2) using MBM. Each node is equipped with n_r receive antennas, and one transmit antenna surrounded by m_{rf} RF mirrors as shown in Fig. 1. An m_{rf}-length pattern of ON/OFF status of the m_{rf} mirrors is called as the 'mirror activation pattern (MAP)'. Since each mirror can be either ON or OFF, a total of $2^{m_{rf}}$ MAPs are possible. Each of these MAPs results in a different realization of the channel, resulting in a MBM channel alphabet of size $N_m \triangleq 2^{m_{rf}}$. Therefore, the index of the chosen MAP in a given channel use conveys m_{rf} information bits (referred to as 'MAP index bits'). A mapping is done between the combinations of m_{rf} information bits and the MAPs. This mapping is made known a priori to both transmitter of node i and receiver of node j, $j = \{1,2\} \setminus i$, for encoding and decoding purposes, respectively. In addition to the m_{rf} bits conveyed through the choice of a MAP in a given channel use, a symbol from a conventional modulation alphabet $\mathbb{A}$ (e.g., QAM/PSK) transmitted by the antenna also conveys information bits (referred to as 'modulation symbol bits'). Let $M \triangleq |\mathbb{A}|$. The achieved rate in FD-MBM, in bits per channel use (bpcu) per node, is then given by

$$\eta_{\text{fd-mbm}} = \underbrace{m_{rf}}_{\text{MAP index bits}} + \underbrace{\log_2 M}_{\text{modulation symbol bits}} \text{ bpcu per node.} \quad (1)$$

Therefore, the FD-MBM system can exchange $\eta_{\text{sys-1}} = 2\eta_{\text{fd-mbm}} = 2(m_{rf}+\log_2 M)$ bits between the two nodes in each channel use. The FD-MBM transmitter at node i, $i = 1, 2$, is shown in Fig. 2. In each channel use, the transmitter takes $m_{rf} + \log_2 M$ bits and encode them as follows. The m_{rf} bits are mapped to a MAP index $l_i, 1 \le l_i \le N_m$, and the remaining $\log_2 M$ bits are mapped to a modulation symbol $s_i \in \mathbb{A}$. The transmit antenna transmits the symbol s_i and the RF mirrors are activated (made ON/OFF) as per the l_ith MAP.

A. Received signal

Let $\mathbf{h}_{ij}^k = [h_{ij}^{1k}\ h_{ij}^{2k}\ \cdots\ h_{ij}^{n_r k}]^T$ denote the $n_r \times 1$ channel gain vector corresponding to the kth MAP of node i to the receiver of node j, where h_{ij}^{lk} is the channel fade coefficient corresponding to the kth MAP of node i to the lth receive antenna of node j, $i = 1, 2$, $j = 1, 2$, $l = 1, 2, \cdots, n_r$, and $k = 1, 2, \cdots, N_m$. Let $\mathbb{H}_{ij} = \{\mathbf{h}_{ij}^1, \mathbf{h}_{ij}^2, \cdots, \mathbf{h}_{ij}^{N_m}\}$, $i = 1, 2$, $j = 1, 2$, be the MBM channel alphabet from node i to node j corresponding to these channel gain vectors. Note that $|\mathbb{H}_{ij}| = N_m = 2^{m_{rf}}$ for every i, j. Let $\mathbf{H}_{ij}$ denote the $n_r \times N_m$ channel matrix from node i to node j, which is given by $\mathbf{H}_{ij} = [\mathbf{h}_{ij}^1\ \mathbf{h}_{ij}^2\ \cdots\ \mathbf{h}_{ij}^{N_m}]$, $i = 1, 2$, $j = 1, 2$. We refer to $\mathbb{H}_{ij}$ and $\mathbf{H}_{ij}$ as the 'desired channel alphabet' and 'desired channel matrix', respectively, when $i \neq j$. Similarly, we refer to $\mathbb{H}_{ij}$ and $\mathbf{H}_{ij}$ as the 'self-interference (SI) channel alphabet' and 'SI channel matrix', respectively, when $i = j$. These channel alphabets are estimated a priori at the receivers through pilot transmissions.

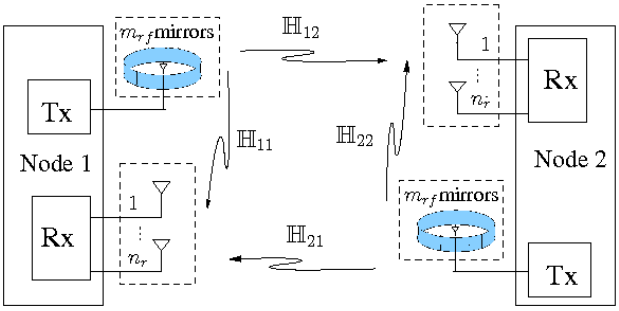

Fig. 1. Full-duplex MBM scheme.

Channel correlation model: The entries of the desired channel matrices $\mathbf{H}_{ij}, i \neq j$, are assumed to be independent and identically distributed (i.i.d.) and distributed as $\mathcal{CN}(0,1)$ as in [16]-[21]. The entries of the SI channel matrices $\mathbf{H}_{ii}, i = 1, 2$ are distributed as $\mathcal{CN}(0,1)$ by assuming that the line-of-sight component is removed by SI cancellation [11]. However, the entries of $\mathbf{H}_{ii}, i = 1, 2$ can be correlated due to space limitation between the transmit and receive antennas. We consider the Kronecker model to account for these spatial correlations. The SI channel matrix $\mathbf{H}_{ii}$ is then given by $\mathbf{H}_{ii} = \mathbf{R}_r^{1/2}\tilde{\mathbf{H}}_{ii}\mathbf{R}_m^{1/2}$, where $\mathbf{R}_r$ is the $n_r \times n_r$ receive correlation matrix, $\tilde{\mathbf{H}}_{ii}$ is a matrix of size $n_r \times N_m$ whose entries are i.i.d. and distributed as $\mathcal{CN}(0,1)$, and $\mathbf{R}_m$ is the $N_m \times N_m$ MAP correlation matrix. We assume receive correlation is zero as in [7], i.e., $\mathbf{R}_r = \mathbf{I}_{n_r}$, where $\mathbf{I}_p$ denotes the identity matrix of size $p \times p$. The equicorrelation model is used to characterize the correlation between fades across MAPs as in [20], i.e., $\mathbf{R}_m = (1-\rho)\mathbf{I}_{N_m} + \rho\mathbf{1}_{N_m}$, where ρ denotes the correlation coefficient in the equicorrelation model and $\mathbf{1}_p$ denotes the all ones matrix of size $p \times p$.

Now, the $n_r \times 1$ received signal vector $\mathbf{y}_i$ at node i in a given channel use can be written as

$$\begin{aligned}\mathbf{y}_i &= \underbrace{\mathbf{h}_{ji}^{l_j} s_j}_{\text{desired signal}} + \underbrace{\mathbf{h}_{ii}^{l_i} s_i}_{\text{SI signal}} + \mathbf{n}_i \\ &= \mathbf{H}_{ji}\mathbf{e}_{l_j} s_j + \mathbf{H}_{ii}\mathbf{e}_{l_i} s_i + \mathbf{n}_i \\ &= \mathbf{H}_{ji}\mathbf{x}_j + \mathbf{H}_{ii}\mathbf{x}_i + \mathbf{n}_i, \end{aligned} \quad (2)$$

where $j = \{1,2\} \setminus i$, $\mathbf{e}_p$ is an $N_m \times 1$ vector whose pth coordinate is 1 and all other coordinates are zero, $\mathbf{n}_i$ is the $n_r \times 1$ additive noise vector whose elements are i.i.d. and distributed as $\mathcal{CN}(0, \sigma^2)$, $\mathbf{x}_i = s_i\mathbf{e}_{l_i}$, and $\mathbf{x}_j = s_j\mathbf{e}_{l_j}$. Note that the vectors $\mathbf{x}_i$ and $\mathbf{x}_j$ belong to the FD-MBM signal set $\mathbb{S}_{\text{fd-mbm}}$, which is given by

$$\mathbb{S}_{\text{fd-mbm}} = \left\{\mathbf{x} : \mathbf{x} = s\mathbf{e}_l, s \in \mathbb{A},\ l \in \{1, 2, \cdots, N_m\}\right\}. \quad (3)$$

The size of the FD-MBM signal set is $|\mathbb{S}_{\text{fd-mbm}}| = 2^{\eta_{\text{fd-mbm}}} = MN_m$. For example, if $m_{rf} = 2$ and $M = 2$ (i.e., BPSK), then $|\mathbb{S}_{\text{fd-mbm}}| = 8$, and the corresponding FD-MBM signal set is given by

$$\mathbb{S}_{\text{fd-mbm}} = \{\mathbf{e}_1,\ -\mathbf{e}_1,\ \mathbf{e}_2,\ -\mathbf{e}_2,\ \mathbf{e}_3,\ -\mathbf{e}_3,\ \mathbf{e}_4,\ -\mathbf{e}_4\}. \quad (4)$$

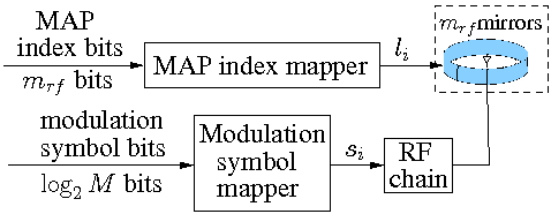

Fig. 2. FD-MBM transmitter at node i, $i = 1, 2$.

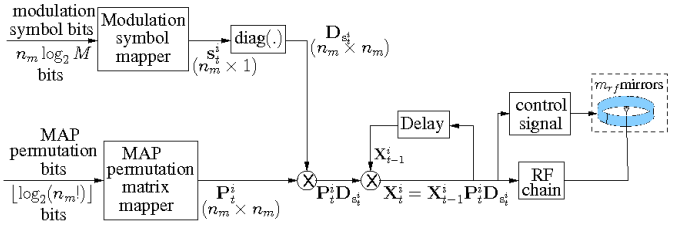

Fig. 3. FD-DMBM transmitter at node i, $i = 1, 2$.

Note that $\mathbf{x}_i$ is perfectly known to node i. Assuming full CSI is available at the receiver of node i, i.e., channel matrices $\mathbf{H}_{ji}$, $j = 1, 2$, the ML decision rule is given by

$$\hat{\mathbf{x}}_j = \underset{\mathbf{x} \in \mathbb{S}_{\text{fd-mbm}}}{\operatorname{argmin}} \|\mathbf{y}_i - \mathbf{H}_{ii}\mathbf{x}_i - \mathbf{H}_{ji}\mathbf{x}\|^2. \tag{5}$$

The non-zero entry in $\hat{\mathbf{x}}_j$ is demapped to get $\log_2 M$ modulation symbol bits and the index of the non-zero location in $\hat{\mathbf{x}}_j$ is demapped to get m_{rf} MAP index bits.

III. FD-DMBM SYSTEM

In this section, we relax the full CSI assumption by considering differential MBM [22] for FD operation with no CSI/partial CSI. We present the full-duplex differential MBM (FD-DMBM) signaling scheme and propose schemes for the detection of FD-DMBM signals.

A. Transmitter

The FD-DMBM transmitter at node i, $i = 1, 2$, is shown in Fig. 3. It uses only n_m MAPs out of the available N_m MAPs for transmission, $1 \le n_m \le N_m$. The transmission takes place block-wise over n_m channel uses. Let the tth block consist of channel uses $tn_m + 1$ to $(t+1)n_m$. In the tth transmission block, the transmitter takes $n_m \log_2 M + \lfloor \log_2(n_m!) \rfloor$ bits and encodes them as follows. The $n_m \log_2 M$ bits are mapped to a modulation symbol vector $\mathbf{s}_t^i \in \mathbb{A}^{n_m}$, where $\mathbb{A}$ denotes an M-ary PSK alphabet. The $\lfloor \log_2(n_m!) \rfloor$ bits are mapped to a MAP permutation matrix $\mathbf{P}_t^i$ of size $n_m \times n_m$ such that the matrix $\mathbf{P}_t^i$ has only one non-zero element $(= 1)$ in each row and in each column, i.e., $\mathbf{P}_t^i$ is of the form $\mathbf{P}_t^i = [\mathbf{g}_{l_t^{i_1}} \ \mathbf{g}_{l_t^{i_2}} \ \dots \ \mathbf{g}_{l_t^{i_{n_m}}}]$, $1 \le b, c, l_t^{i_b}, l_t^{i_c} \le n_m$, $l_t^{i_b} \ne l_t^{i_c}$ $\forall\ b \ne c$, $\mathbf{g}_p$ is an $n_m \times 1$ vector whose pth coordinate is 1 and all other coordinates are zero, and $l_t^{i_b}$ denotes the index of the selected MAP in the $(tn_m + b)$th channel use at node i. Note that each MAP is selected only once in a block. The achieved rate in FD-DMBM in bpcu per node is given by

$$\eta_{\text{fd-dmbm}} = \underbrace{\log_2 M}_{\substack{\text{modulation} \\ \text{symbol bits}}} + \underbrace{\frac{1}{n_m}\lfloor \log_2(n_m!) \rfloor}_{\text{MAP permutation bits}} \text{ bpcu per node.} \tag{6}$$

Therefore, the FD-DMBM system can exchange $\eta_{\text{sys-2}} = 2n_m\eta_{\text{fd-dmbm}} = 2(\lfloor \log_2(n_m!) \rfloor + n_m \log_2 M)$ bits between the two nodes over each transmission block. The transmission matrix in the tth block is of size $n_m \times n_m$, denoted by $\mathbf{X}_t^i$, is generated in a differential manner as

$$\mathbf{X}_t^i = \mathbf{X}_{t-1}^i \mathbf{P}_t^i \mathbf{D}_{\mathbf{s}_t^i}, \ i = 1, 2. \tag{7}$$

where $\mathbf{D}_{\mathbf{s}_t^i} = \text{diag}(\mathbf{s}_t^i)$, $\mathbf{X}_0^i = \mathbf{P}_0^i \mathbf{D}_{\mathbf{s}_0^i}$, $\mathbf{P}_0^i$ can be any arbitrary MAP permutation matrix, and $\mathbf{s}_0^i$ can be any arbitrary vector in $\mathbb{A}^{n_m}$. Without loss of generality, we assume $\mathbf{P}_0 = \mathbf{I}_{n_m}$ and $\mathbf{s}_0$ is a vector of all ones. Note that for any t, $\mathbf{X}_t^i$ can have only one non-zero element belonging to $\mathbb{A}$ in each row and in each column. Let $x_{l_t^{i_b}, b}$, the $(l_t^{i_b}, b)$th entry of $\mathbf{X}_t^i$, be the non-zero element belonging to $\mathbb{A}$. Then, in the $(tn_m + b)$th channel use, the transmit antenna transmits the symbol $x_{l_t^{i_b}, b}$ and the RF mirrors are activated as per the $l_t^{i_b}$th MAP.

B. FD-DMBM signal set

A total of $n_m!$ MAP permutation matrices are possible. Out of them, $2^{\lfloor \log_2 (n_m!) \rfloor}$ matrices are chosen to form a set of MAP permutation matrices, denoted by $\mathbb{P}$. The FD-DMBM signal set, denoted by $\mathbb{S}_{\text{fd-dmbm}}$, is given by

$$\mathbb{S}_{\text{fd-dmbm}} = \big\{ \{\mathbf{P}, \mathbf{s}\} : \mathbf{P} \in \mathbb{P}, \mathbf{s} \in \mathbb{A}^{n_m} \big\}. \tag{8}$$

Note that $\forall\ \{\mathbf{P}, \mathbf{s}\} \in \mathbb{S}_{\text{fd-dmbm}}$, $\mathbf{P}\mathbf{D}_\mathbf{s}\mathbf{D}_\mathbf{s}^\dagger\mathbf{P}^\dagger = \mathbf{D}_\mathbf{s}^\dagger\mathbf{P}^\dagger\mathbf{P}\mathbf{D}_\mathbf{s} = \mathbf{I}_{n_m}$, where $(.)^\dagger$ denotes the conjugate transpose.

Example 1: For $n_m = 2$ and BPSK, the bpcu per node is 1.5, and the set $\mathbb{P}$ is given by

$$\mathbb{P} = \big\{ [\mathbf{g}_1 \ \ \mathbf{g}_2], [\mathbf{g}_2 \ \ \mathbf{g}_1] \big\} = \Bigg\{ \underbrace{\begin{bmatrix} 1 & 0 \\ 0 & 1 \end{bmatrix}}_{\triangleq \mathbf{P}_1}, \underbrace{\begin{bmatrix} 0 & 1 \\ 1 & 0 \end{bmatrix}}_{\triangleq \mathbf{P}_2} \Bigg\}. \tag{9}$$

The corresponding FD-DMBM signal set $\mathbb{S}_{\text{fd-dmbm}}$ is given by

$$\begin{aligned} \mathbb{S}_{\text{fd-dmbm}} = \Big\{ &\{\mathbf{P}_1, [1\ 1]^T\}, \{\mathbf{P}_1, [1\ -1]^T\}, \{\mathbf{P}_1, [-1\ 1]^T\}, \\ &\{\mathbf{P}_1, [-1\ -1]^T\}, \{\mathbf{P}_2, [1\ 1]^T\}, \{\mathbf{P}_2, [1\ -1]^T\}, \\ &\{\mathbf{P}_2, [-1\ 1]^T\}, \{\mathbf{P}_2, [-1\ -1]^T\} \Big\}. \end{aligned} \tag{10}$$

The transmitter takes three bits at a time and encode them as follows; the first bit is used to choose one among $\mathbf{P}_1$ and $\mathbf{P}_2$ as $\mathbf{P}_t^i$, and the remaining two bits are used to choose the $\mathbf{s}_t^i$ vector from $\mathbb{A}^{n_m}$. The resulting $\mathbf{X}_t^i$ matrix of size 2×2 generated as per (7) is then sent in two consecutive channel uses $2t + 1$ and $2(t + 1)$.

C. Received signal

Let $\mathbf{H}_{ij}$, $i = 1, 2$, $j = 1, 2$, denote the $n_r \times n_m$ channel matrix from node i to node j defined as in Sec. II. Assuming quasi-static channel over three adjacent block intervals, the $n_r \times n_m$ received signal blocks $\mathbf{Y}_{t-2}^i$, $\mathbf{Y}_{t-1}^i$, and $\mathbf{Y}_t^i$ at node i in the $(t-2)$th, $(t-1)$th, and tth block intervals, respectively, are given by

$$\mathbf{Y}^i_{t-2} = \underbrace{\mathbf{H}_{ji}\mathbf{X}^j_{t-2}}_{\text{desired signal}} + \underbrace{\mathbf{H}_{ii}\mathbf{X}^i_{t-2}}_{\text{SI signal}} + \mathbf{N}^i_{t-2}, \quad (11)$$

$$\mathbf{Y}^i_{t-1} = \mathbf{H}_{ji}\mathbf{X}^j_{t-1} + \mathbf{H}_{ii}\mathbf{X}^i_{t-1} + \mathbf{N}^i_{t-1}, \quad (12)$$

$$\mathbf{Y}^i_{t} = \mathbf{H}_{ji}\mathbf{X}^j_{t} + \mathbf{H}_{ii}\mathbf{X}^i_{t} + \mathbf{N}^i_{t}, \quad (13)$$

where $j = \{1,2\} \setminus i$, $\mathbf{N}^i_{t-2}$, $\mathbf{N}^i_{t-1}$, and $\mathbf{N}^i_t$ are the additive noise matrices of size $n_r \times n_m$ in the $(t-2)$th, $(t-1)$th, and tth block intervals, respectively, whose elements i.i.d. and distributed as $\mathcal{CN}(0,\sigma^2)$.

Now, we present three types of detectors for FD-DMBM signal detection, namely, 1) desired channel-aware (DCA) detector that requires only the desired channel matrix at the receiver, which is a commonly used detector for SI cancellation [14],[15], 2) SI channel-aware (SICA) detector that requires only the SI channel matrix at the receiver, and 3) channel-unaware (CU) detector that does not need any channel matrix at the receiver for detection.

1) DCA detector: Post-multiplying (12) with $\mathbf{P}^i_t\mathbf{D}_{\mathbf{s}^i_t}$ and substituting (7), we have

$$\mathbf{Y}^i_{t-1}\mathbf{P}^i_t\mathbf{D}_{\mathbf{s}^i_t} = \mathbf{H}_{ji}\mathbf{X}^j_{t-1}\mathbf{P}^i_t\mathbf{D}_{\mathbf{s}^i_t} + \mathbf{H}_{ii}\mathbf{X}^i_t + \mathbf{N}^i_{t-1}\mathbf{P}^i_t\mathbf{D}_{\mathbf{s}^i_t}. \quad (14)$$

From (13) and (14), we have

$$\mathbf{Y}^i_t = \mathbf{Y}^i_{t-1}\mathbf{P}^i_t\mathbf{D}_{\mathbf{s}^i_t} + \mathbf{H}_{ji}\mathbf{X}^j_{t-1}\big(\mathbf{P}^j_t\mathbf{D}_{\mathbf{s}^j_t} - \mathbf{P}^i_t\mathbf{D}_{\mathbf{s}^i_t}\big) + \tilde{\mathbf{N}}^i_{t,d}, \quad (15)$$

where $\tilde{\mathbf{N}}^i_{t,d} = \mathbf{N}^i_t - \mathbf{N}^i_{t-1}\mathbf{P}^i_t\mathbf{D}_{\mathbf{s}^i_t}$. We can see that the elements of $\tilde{\mathbf{N}}^i_{t,d}$ are i.i.d. and distributed as $\mathcal{CN}(0,2\sigma^2)$. Note that (15) depends not only on $\{\mathbf{P}^j_t, \mathbf{s}^j_t\}$, but also on the previous transmitted block $\mathbf{X}^j_{t-1}$. Therefore, optimal detection requires joint detection across the blocks $\{\mathbf{P}^j_u, \mathbf{s}^j_u\}^t_{u=1}$, whose computational complexity grows exponentially in t. So, instead of optimal detection, we consider a sub-optimal detection scheme whose decision rule is given by

$$\{\hat{\mathbf{P}}^j_t, \hat{\mathbf{s}}^j_t\} = \underset{\{\mathbf{P}^j_t,\mathbf{s}^j_t\}\in\mathbb{S}_{\text{fd-dmbm}}}{\text{argmax}} P\Big(\mathbf{Y}^i_{t-1}, \mathbf{Y}^i_{t-1}/\{\mathbf{P}^j_t, \mathbf{s}^j_t\}, \hat{\mathbf{X}}^j_{t-1}\Big)$$
$$= \underset{\{\mathbf{P}^j_t,\mathbf{s}^j_t\}\in\mathbb{S}_{\text{fd-dmbm}}}{\text{argmin}} \|\mathbf{Y}^i_{t,\text{dca}} - \mathbf{H}_{ji}\hat{\mathbf{X}}^j_{t-1}\mathbf{P}^j_t\mathbf{D}_{\mathbf{s}^j_t}\|^2, \quad (16)$$

where $\mathbf{Y}^i_{t,\text{dca}} = \mathbf{Y}^i_t - \mathbf{Y}^i_{t-1}\mathbf{P}^i_t\mathbf{D}_{\mathbf{s}^i_t} + \mathbf{H}_{ji}\hat{\mathbf{X}}^j_{t-1}\mathbf{P}^i_t\mathbf{D}_{\mathbf{s}^i_t}$, and $\hat{\mathbf{X}}^j_{t-1}$ denotes the estimate of the $(t-1)$th transmitted block, which is given by $\hat{\mathbf{X}}^j_{t-1} = \mathbf{P}^j_0\mathbf{D}_{\mathbf{s}^j_0}\hat{\mathbf{P}}^j_1\mathbf{D}_{\hat{\mathbf{s}}^j_1}\cdots\hat{\mathbf{P}}^j_{t-1}\mathbf{D}_{\hat{\mathbf{s}}^j_{t-1}}$, assuming zeroth transmitted block $\{\mathbf{P}^j_0, \mathbf{D}_{\mathbf{s}^j_0}\}$ by node j is perfectly known at node i.

2) SICA detector: Post-multiplying (12) with $\mathbf{P}^j_t\mathbf{D}_{\mathbf{s}^j_t}$ and substituting (7), we have

$$\mathbf{Y}^i_{t-1}\mathbf{P}^j_t\mathbf{D}_{\mathbf{s}^j_t} = \mathbf{H}_{ji}\mathbf{X}^j_t + \mathbf{H}_{ii}\mathbf{X}^i_{t-1}\mathbf{P}^j_t\mathbf{D}_{\mathbf{s}^j_t} + \mathbf{N}^i_{t-1}\mathbf{P}^j_t\mathbf{D}_{\mathbf{s}^j_t}. \quad (17)$$

From (13) and (17), we have

$$\mathbf{Y}^i_t = \mathbf{Y}^i_{t-1}\mathbf{P}^j_t\mathbf{D}_{\mathbf{s}^j_t} + \mathbf{H}_{ii}\mathbf{X}^i_{t-1}\big(\mathbf{P}^i_t\mathbf{D}_{\mathbf{s}^i_t} - \mathbf{P}^j_t\mathbf{D}_{\mathbf{s}^j_t}\big) + \tilde{\mathbf{N}}^i_{t,s}, \quad (18)$$

where $\tilde{\mathbf{N}}^i_{t,s} = \mathbf{N}^i_t - \mathbf{N}^i_{t-1}\mathbf{P}^j_t\mathbf{D}_{\mathbf{s}^j_t}$. Note that the elements of $\tilde{\mathbf{N}}^i_{t,s}$ are i.i.d. and distributed as $\mathcal{CN}(0,2\sigma^2)$. The ML decision rule is given by

$$\{\hat{\mathbf{P}}^j_t, \hat{\mathbf{s}}^j_t\} = \underset{\{\mathbf{P}^j_t,\mathbf{s}^j_t\}\in\mathbb{S}_{\text{fd-dmbm}}}{\text{argmin}} \|\mathbf{Y}^i_{t,\text{sca}_1} - \mathbf{Y}^i_{t,\text{sca}_2}\mathbf{P}^j_t\mathbf{D}_{\mathbf{s}^j_t}\|^2, \quad (19)$$

where $\mathbf{Y}^i_{t,\text{sca}_1} = \mathbf{Y}^i_t - \mathbf{H}_{ii}\mathbf{X}^i_t$ and $\mathbf{Y}^i_{t,\text{sca}_2} = \mathbf{Y}^i_{t-1} - \mathbf{H}_{ii}\mathbf{X}^i_{t-1}$. Note that the SICA detector does not need node j's zeroth transmitted block at node i.

3) CU detector: Applying the same steps of SICA detector on (11) and (12), we have

$$\mathbf{Y}^i_{t-1} = \mathbf{Y}^i_{t-2}\mathbf{P}^j_{t-1}\mathbf{D}_{\mathbf{s}^j_{t-1}} + \mathbf{H}_{ii}\mathbf{X}^i_{t-2}\big(\mathbf{P}^i_{t-1}\mathbf{D}_{\mathbf{s}^i_{t-1}} - \mathbf{P}^j_{t-1}\mathbf{D}_{\mathbf{s}^j_{t-1}}\big) + \tilde{\mathbf{N}}^i_{t-1,s}, \quad (20)$$

where $\tilde{\mathbf{N}}^i_{t-1,s} = \mathbf{N}^i_{t-1} - \mathbf{N}^i_{t-2}\mathbf{P}^j_{t-1}\mathbf{D}_{\mathbf{s}^j_{t-1}}$. Assuming that $\big(\mathbf{P}^i_{t-1}\mathbf{D}_{\mathbf{s}^i_{t-1}} - \mathbf{P}^j_{t-1}\mathbf{D}_{\mathbf{s}^j_{t-1}}\big)$ is invertible, (20) can be written as

$$\mathbf{H}_{ii}\mathbf{X}^i_{t-2} = \Big(\mathbf{Y}^i_{t-1} - \mathbf{Y}^i_{t-2}\mathbf{P}^j_{t-1}\mathbf{D}_{\mathbf{s}^j_{t-1}} - \tilde{\mathbf{N}}^i_{t-1,s}\Big) \times \big(\mathbf{P}^i_{t-1}\mathbf{D}_{\mathbf{s}^i_{t-1}} - \mathbf{P}^j_{t-1}\mathbf{D}_{\mathbf{s}^j_{t-1}}\big)^{-1}. \quad (21)$$

Substituting (21) in (18) and simplifying, we get

$$\mathbf{Y}^i_t = \mathbf{Y}^i_{t-1}\mathbf{A}^i_t - \mathbf{Y}^i_{t-2}\mathbf{B}^i_t + \mathbf{N}^i_{t,\text{cu}}, \quad (22)$$

where

$$\mathbf{A}^i_t = \big(\mathbf{P}^i_{t-1}\mathbf{D}_{\mathbf{s}^i_{t-1}} - \mathbf{P}^j_{t-1}\mathbf{D}_{\mathbf{s}^j_{t-1}}\big)^{-1} \times \big(\mathbf{P}^i_{t-1}\mathbf{D}_{\mathbf{s}^i_{t-1}}\mathbf{P}^i_t\mathbf{D}_{\mathbf{s}^i_t} - \mathbf{P}^j_{t-1}\mathbf{D}_{\mathbf{s}^j_{t-1}}\mathbf{P}^j_t\mathbf{D}_{\mathbf{s}^j_t}\big), \quad (23)$$

$$\mathbf{B}^i_t = \mathbf{P}^j_{t-1}\mathbf{D}_{\mathbf{s}^j_{t-1}}\big(\mathbf{P}^i_{t-1}\mathbf{D}_{\mathbf{s}^i_{t-1}} - \mathbf{P}^j_{t-1}\mathbf{D}_{\mathbf{s}^j_{t-1}}\big)^{-1} \times \mathbf{P}^i_{t-1}\mathbf{D}_{\mathbf{s}^i_{t-1}}\big(\mathbf{P}^i_t\mathbf{D}_{\mathbf{s}^i_t} - \mathbf{P}^j_t\mathbf{D}_{\mathbf{s}^j_t}\big), \quad (24)$$

and $\mathbf{N}^i_{t,\text{cu}} = \mathbf{N}^i_t - \mathbf{N}^i_{t-1}\mathbf{A}^i_t + \mathbf{N}^i_{t-2}\mathbf{B}^i_t$. Let $\mathbf{n}^{i,p}_{t,cu}$ denote the pth row of $\mathbf{N}^i_{t,\text{cu}}$, $p = 1,2,\cdots,n_r$. We can see that $\mathbf{n}^{i,p}_{t,cu}$ is a complex Gaussian random vector with

$$\mathbb{E}(\mathbf{n}^{i,p}_{t,cu}) = \mathbf{0}_{1\times n_m},$$
$$\mathbb{E}[(\mathbf{n}^{i,p}_{t,cu})^\dagger \mathbf{n}^{i,q}_{t,cu}] = \begin{cases} \mathbf{C}^i_t & \text{if } p = q \\ \mathbf{0}_{n_m\times n_m} & \text{if } p \neq q \end{cases}, \quad (25)$$

where $\mathbf{C}^i_t = \sigma^2\Big(\mathbf{I}_{n_m} + (\mathbf{A}^i_t)^\dagger\mathbf{A}^i_t + (\mathbf{B}^i_t)^\dagger\mathbf{B}^i_t\Big)$, $\mathbb{E}(.)$ denotes the expectation operator, and $\mathbf{0}_{u\times v}$ denotes the all-zero matrix of size $u \times v$. Therefore, the ML decision rule is given by

$$\big\{\{\hat{\mathbf{P}}^j_u, \hat{\mathbf{s}}^j_u\}\big\}^t_{u=t-1} = \underset{\big\{\{\mathbf{P}^j_u,\mathbf{s}^j_u\}\big\}^t_{u=t-1}\in\mathbb{S}_{\text{fd-dmbm}}}{\text{argmin}} \mathcal{C}\big(\{\mathbf{P}^j_u, \mathbf{s}^j_u\}\big), \quad (26)$$

where $\mathcal{C}\big(\{\mathbf{P}^j_u, \mathbf{s}^j_u\}\big) = \text{Tr}[\mathbf{Y}^i_{t,\text{c}}(\mathbf{C}^i_t)^{-1}(\mathbf{Y}^i_{t,\text{c}})^\dagger] + n_r\log(\det(\mathbf{C}^i_t))$, $\mathbf{Y}^i_{t,\text{c}} = \mathbf{Y}^i_t - \mathbf{Y}^i_{t-1}\mathbf{A}^i_t + \mathbf{Y}^i_{t-2}\mathbf{B}^i_t$, and Tr(.) denotes the trace operator. Note that the CU detector jointly detects $(t-1)$th and tth block information bits at the tth block. In other words, the CU detector operates once in two transmission blocks (i.e., at $(2p)$th transmission block, $p = 1,2,\cdots$). We now present a mapping rule from the information bits to a signal set such that $(\mathbf{A}^i_t, \mathbf{B}^i_t)$ is unique and $\big(\mathbf{P}^i_{t-1}\mathbf{D}_{\mathbf{s}^i_{t-1}} - \mathbf{P}^j_{t-1}\mathbf{D}_{\mathbf{s}^j_{t-1}}\big)$ is invertible.

Signal set mapping: Both nodes use Lehmer code [23] to map the MAP permutation bits to a MAP permutation matrix. Node 1 maps its modulation symbol bits to conventional M-PSK modulation symbols (without any rotation, i.e., $\mathbb{A}$). To make $\big(\mathbf{P}^i_{t-1}\mathbf{D}_{\mathbf{s}^i_{t-1}} - \mathbf{P}^j_{t-1}\mathbf{D}_{\mathbf{s}^j_{t-1}}\big)$ invertible, node 2 maps its modulation symbol bits to a rotated M-PSK symbols in the

$(t-1)$th transmission block (i.e., in $(2p-1)$th transmission block, $p = 1, 2, \cdots$). The modulation symbol vector $\mathbf{s}_{t-1}^2$ takes its qth element from the set $\mathbb{A}_q$, which is given by $\mathbb{A}_q = \exp(\imath \frac{\pi}{(2^{q-1})M})\mathbb{A}$, $q = 1, 2, \cdots, n_m$, where $\imath = \sqrt{-1}$. Further, to make the pair $(\mathbf{A}_t^i, \mathbf{B}_t^i)$ unique, the modulation symbol vector $\mathbf{s}_t^2$ in tth transmission block (i.e., in $(2p)$th transmission block, $p = 1, 2, \cdots$) takes its elements from $\mathbb{A}_{n_m}$. Note that there can be other mappings are also possible to make $(\mathbf{A}_t^i, \mathbf{B}_t^i)$ is unique and $\left(\mathbf{P}_{t-1}^i \mathbf{D}_{\mathbf{s}_{t-1}^i} - \mathbf{P}_{t-1}^j \mathbf{D}_{\mathbf{s}_{t-1}^j}\right)$ is invertible.

After detection, the vector $\hat{\mathbf{s}}_t^j$ is demapped to get $n_m \log_2 M$ modulation symbol bits, and the matrix $\hat{\mathbf{P}}_t^j$ is demapped to get $\lfloor \log_2(n_m!) \rfloor$ MAP permutation bits.

IV. Results and Discussions

In this section, we present the bit error rate (BER) performance of FD-MBM and FD-DMBM schemes as a function of average signal-to-noise ratio (SNR). The average SNR is defined as E_s/σ^2, where E_s denotes the average energy of QAM/PSK modulation alphabet.

In Fig. 4, we present a comparison between the BER performance of FD-MBM and FD with conventional modulation (FD-CM) schemes. All the schemes considered in this figure use $n_r = 2$, ML detection, and convey 4 bpcu per node. The following schemes are considered. FD-MBM schemes: *i)* $m_{rf} = 2$, 4-QAM; *ii)* $m_{rf} = 1$, 8-QAM/8-PSK. FD-CM schemes: 16-QAM/16-PSK. It is seen that FD-MBM schemes achieve better performance compared to FD-CM schemes. For example, at 10^{-4} BER, FD-MBM with $m_{rf} = 2$ and 4-QAM requires about 2 dB and 4.5 dB less SNR compared to FD-CM with 16-QAM and 16-PSK, respectively. Similarly, FD-MBM with $m_{rf} = 1$ and 8-PSK performs better than FD-CM with 16-QAM and 16-PSK by about 1 dB and 3.5 dB, respectively. A reason for this performance advantage is the use of a smaller sized modulation alphabet in FD-MBM (4-QAM, 8-PSK) compared to FD-CM (16-QAM, 16-PSK). It is also seen that both the FD-MBM with 8-QAM and FD-CM using 16-QAM achieve nearly same performance even though FD-MBM uses a smaller sized alphabet. This is because, in this case, the performance gain provided by the smaller sized alphabet is neutralized by the error performance of the MAP index bit. Next, for the same systems considered in Fig. 4, Fig. 5 shows the effect of increasing n_r on the average SNR required to achieve a target BER of 10^{-3}. It is seen that the required SNR in all the systems decreases as n_r is increased. Also, comparative performance similar to that in Fig. 4 can be observed in Fig. 5 as well. For example, FD-MBM with $m_{rf} = 2$ and 4-QAM achieves 10^{-3} BER at 10 dB SNR with $n_r = 4$, whereas FD-CM with 16-QAM and 16-PSK requires $n_r = 7$ and 13, respectively.

Figure 6 shows the BER performance of FD-MBM and FD-DMBM schemes. The following system parameters are considered. FD-MBM: $m_{rf} = 1$, BPSK, 2 bpcu per node, ML detector. FD-DMBM: *i)* $m_{rf} = 1$, $n_m = 2$, BPSK, 1.5 bpcu per node, *ii)* $m_{rf} = 1$, $n_m = 2$, 4-PSK, 2.5 bpcu per node, with DCA, SICA, and CU detectors for FD-DMBM. All the

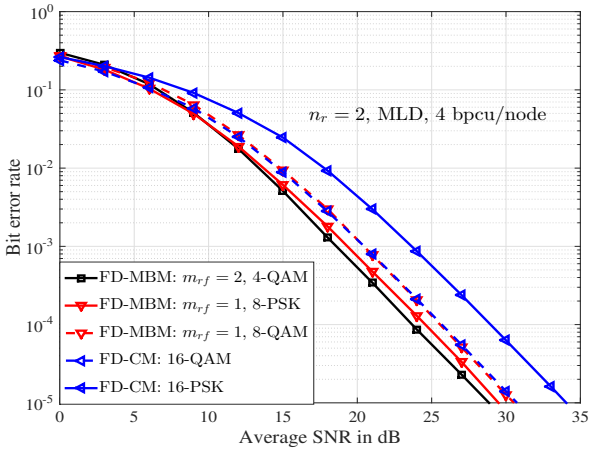

Fig. 4. BER performance of FD-MBM and FD-CM schemes with 4 bpcu per node, $n_r = 2$, and ML detection. FD-MBM: *i)* $m_{rf} = 2$, 4-QAM; *ii)* $m_{rf} = 1$, 8-QAM/8-PSK. FD-CM: 16-QAM/16-PSK.

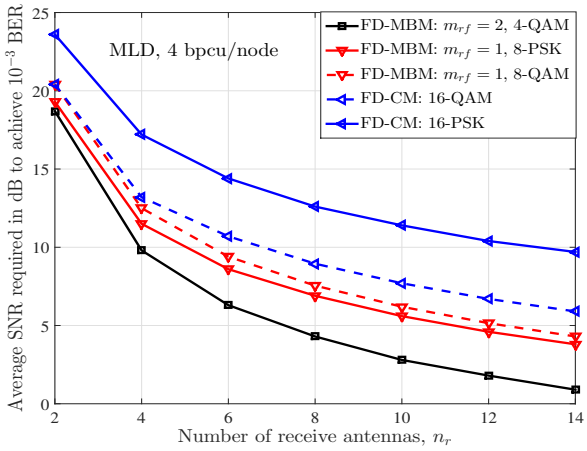

Fig. 5. Average SNR required to achieve 10^{-3} BER in FD-MBM and FD-CM schemes.

schemes use $n_r = 2$ and $\rho = 0$ (i.e., no correlation between the SI channel fades corresponding to different MAPs). It is seen that FD-MBM achieves better performance among all the schemes. This is because of the availability of full CSI at the receiver for detection in FD-MBM. It is also seen that the performance loss in FD-DMBM with 1.5 bpcu per node and 2.5 bpcu per node using SICA detector compared to FD-MBM with 2 bpcu per node using ML detector is about 0.5 dB and 2.5 dB, respectively. Similarly, the performance loss in FD-DMBM with 1.5 bpcu per node and 2.5 bpcu per node using CU detector (which does not need any CSI) compared to FD-MBM with 2 bpcu per node using ML detector (which needs full CSI) is about 8.5 dB and 13.5 dB, respectively. It is further seen that, at given spectral efficiency, SICA detector performs better than DCA detector, although both the detectors require only one channel matrix (i.e., desired channel matrix in DCA detector and SI channel matrix in SICA detector) for detection. This is because the DCA detector uses the estimate of the previous transmitted block to detect current information block, which, in turn, results in error propagation. Whereas,

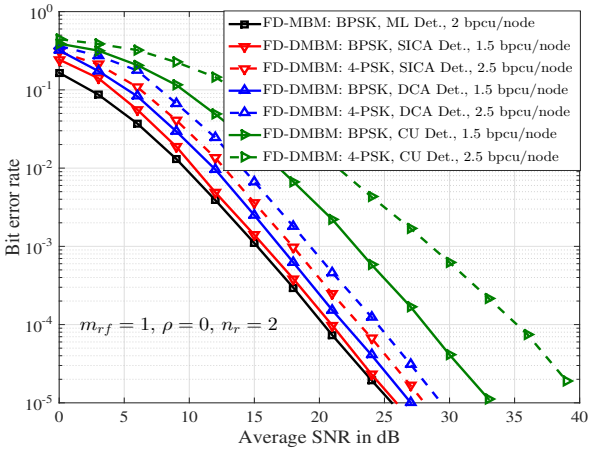

Fig. 6. BER performance of FD-MBM and FD-DMBM schemes with $m_{rf} = 1$, $n_r = 2$, and $\rho = 0$. FD-MBM: BPSK, 2 bpcu per node, ML detector; FD-DMBM: *i*) $n_m = 2$, BPSK, 1.5 bpcu per node; *ii*) $n_m = 2$, 4-PSK, 2.5 bpcu per node; DCA, SICA, and CU detectors for FD-DMBM.

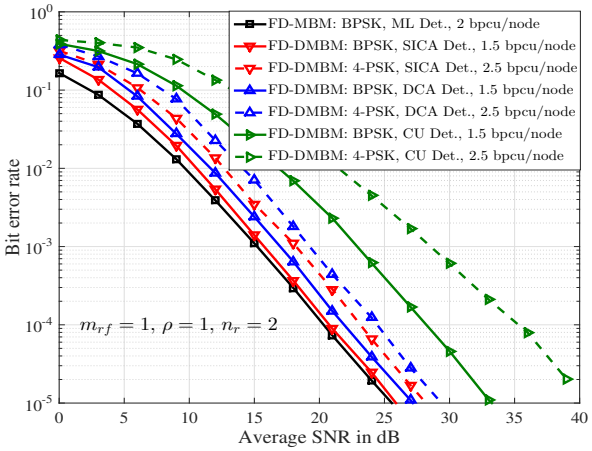

Fig. 7. BER performance of FD-MBM and FD-DMBM schemes with $m_{rf} = 1$, $n_r = 2$, and $\rho = 1$. FD-MBM: BPSK, 2 bpcu per node, ML detector; FD-DMBM: *i*) $n_m = 2$, BPSK, 1.5 bpcu per node; *ii*) $n_m = 2$, 4-PSK, 2.5 bpcu per node; DCA, SICA, and CU detectors for FD-DMBM.

SICA detector does not have this problem of error propagation. Similarly, in Fig. 7, we present the BER performance of the same systems considered in Fig. 6, but with $\rho = 1$, i.e., the SI channel fades corresponding to different MAPs are perfectly correlated. Trends similar to Fig. 6 can be observed in Fig. 7.

V. Conclusions

We introduced and investigated full-duplex communication using media-based modulation. The performance of FD-MBM was shown to be better compared to that of FD communication using conventional modulation with full CSI. Full-duplex communication with differential MBM was studied when no CSI or only partial CSI is available. We proposed detectors for FD-DMBM signal detection; these detectors are (i) DCA detector that requires only the CSI between the two nodes at the receiver, (ii) SICA detector that requires only the self-interference CSI at the receiver, and (iii) CU detector that does not need any CSI at the receiver for detection. As future work, FD-MBM in relaying systems can be investigated.

References

[1] J. I. Choi, M. Jain, K. Srinivasan, P. Levis, and S. Katti, "Achieving single channel full-duplex wireless communication," in *Proc. ACM MobiCom'2010*, Sept. 2010, pp. 1-12.

[2] M. Jain, J. I. Choi, T. M. Kim, D. Bharadia, S. Seth, K. Srinivasan, P. Levis, S. Katti, and P. Sinha, "Practical, real-time, full-duplex wireless," in *Proc. ACM MOBICOM'2011*, Sept. 2011, pp. 301-312.

[3] M. Duarte, C. Dick, and A. Sabharwal, "Experiment-driven characterization of full-duplex wireless systems," *IEEE Trans. Wireless Commun.*, vol. 11, no. 12, pp. 4296-4307, Dec. 2012.

[4] A. Sabharwal, P. Schniter, D. Guo, D. W. Bliss, S. Rangarajan, and R. Wichman, "In-band full-duplex wireless: challenges and opportunities," *IEEE J. Sel. Areas Commun.*, vol. 32, no. 9, pp. 1637-1652, Sept. 2014.

[5] S. Goyal, P. Liu, S. Panwar, R. Difazio, R. Yang, and E. Bala, "Full-duplex cellular systems: will doubling interference prevent doubling capacity?," *IEEE Commun. Mag.*, vol. 53, no. 5, pp. 121-127, May 2015.

[6] Z. Zhang, X. Chai, K. Long, A. V. Vasilakos, and L. Hanzo, "Full-duplex techniques for 5G networks: self-interference cancellation, protocol design, and relay selection," *IEEE Commun. Mag.*, vol. 53, no. 5, pp. 128-137, May 2015.

[7] B. P. Day, A. Margetts, D. W. Bliss, and P. Schniter, "Full-duplex bidirectional MIMO: achievable rates under limited dynamic range," *IEEE Trans. Signal Process.*, vol. 60, no. 7, pp. 3702-3713, Jul. 2012.

[8] I. Krikidis, H. A. Suraweera, P. J. Smith, and C. Yuen, "Full-duplex relay selection for amplify-and-forward cooperative networks," *IEEE Trans. Wireless Commun.*, vol. 11, no. 12, pp. 4381-4393, Dec. 2012.

[9] H. A. Suraweera, I. Krikidis, G. Zheng, C. Yuen, and P. Smith, "Low-complexity end-to-end performance optimization in MIMO full-duplex relay systems," *IEEE Trans. Wireless Commun.*, vol. 13, no. 2, pp. 913-927, Feb. 2014.

[10] L. J. Rodrguez, N. H. Tran, and T. Le-Ngoc, "Performance of full-duplex AF relaying in the presence of residual self-interference," *IEEE J. Sel. Areas Commun.*, vol. 32, no. 9, pp. 1752-1764, Sep. 2014.

[11] G.-P. Liu, R. Yu, H. Ji, V. Leung, and X. Li, "In-band full-duplex relaying: a survey research issues and challenges," *IEEE Commun. Surveys & Tuts.*, vol. 17, no. 2, pp. 500-524, 2015.

[12] I. Krikidis and H. A. Suraweera, "Full-duplex cooperative diversity with Alamouti space-time code," *IEEE Wireless Commun. Lett.*, vol. 2, no. 5, pp. 519-522, Oct. 2013.

[13] B. Jiao, M. Wen, M. Ma, and H. V. Poor, "Spatial modulated full-duplex," *IEEE Wireless Commun. Lett.*, vol. 3, no. 6, pp. 641-644, Dec. 2014.

[14] P. Ju, M. Wen, X. Cheng, and L. Yang, "An effective self-interference cancellation scheme for spatial modulated full-duplex systems," in *Proc. IEEE ICC'2015*, Jun. 2015, pp. 2123-2128.

[15] M. Xu, M. Wen, Y. Feng, F. Ji, and W. Pan, "A novel self-interference cancellation scheme for full-duplex with differential spatial modulation," in *Proc. IEEE PIMRC'2015*, Sept. 2015, pp. 482-486.

[16] A. K. Khandani, "Media-based modulation: a new approach to wireless transmission," in *Proc. IEEE ISIT'2013*, Jul. 2013, pp. 3050-3054.

[17] A. K. Khandani, "Media-based modulation: converting static Rayleigh fading to AWGN," in *Proc. IEEE ISIT'2014*, Jun.-Jul. 2014, pp. 1549-1553.

[18] A. K. Khandani, "Media-based modulation: a new approach to wireless transmission," Univ. Waterloo, Waterloo, ON, Canada. Tech. Rep. [Online]. Available: http://www.cst.uwaterloo.ca/reports/media-report.pdf

[19] E. Seifi, M. Atamanesh, and A. K. Khandani, "Media-based MIMO: outperforming known limits in wireless," in *Proc. IEEE ICC'2016*, May 2016, pp. 1-7.

[20] Y. Naresh and A. Chockalingam, "On media-based modulation using RF mirrors," *IEEE Trans. Veh. Tech.*, vol. 66, no. 6, pp. 4967-4983, Jun. 2017.

[21] B. Shamasundar and A. Chockalingam, "Multiuser media-based modulation for massive MIMO systems," in *Proc. IEEE SPAWC'2017*, Jul. 2017.

[22] Y. Naresh and A. Chockalingam, "A low-complexity maximum-likelihood detector for differential media-based modulation," *IEEE Commun. Lett.*, 2017. IEEE Xplore DOI: 10.1109/LCOMM.2017.2687921.

[23] D. H. Lehmer, "Teaching combinatorial tricks to a computer," in *Proc. Sympos. Appl. Math. Combinatorial Analysis*, 10: 179-193, 1960.